TIME RESOLVED EUV EMISSION OF LASER PRODUCED TIN PLASMAS

P. Hayden, J. Witz[a],C. Fallon, E. T. Kennedy, G. O'Sullivan[b], P. Dunne[b] and J. T. Costello

School of Physical Sciences and National Centre for Plasma Science and Technology, Dublin City University, Glasnevin, Dublin 9, Ireland
[a]Centre de Physique Théorique, École Polytechnique, 91128 Palaiseau, France
[b]School of Physics, University College Dublin, Belfield, Dublin 4, Ireland

Contact: patrick.hayden@dcu.ie

Abstract

To date lithography has been at the forefront of feature size reduction due to the ready availability of intense light sources with ever decreasing wavelength. However, to make further progress new lithography techniques are needed, with extreme ultraviolet lithography, or EUVL, the most promising candidate [1].

One current candidate for the EUVL light source is a tin plasma. Modelling predicts that laser produced tin plasmas, with electron temperatures of 30 to 70 eV, can emit brightly in the desired bandwidth (13.5 nm ± 1%) [2]. Emission in the vicinity of 13.5 nm can be ascribed to overlapping transitions involving the 4d-subshell in Sn^{7+} to Sn^{12+} ions, which merge to form an unresolved transition array (UTA) [3]. We will present time resolved spectra of tin plasma UTA in the 12–16 nm region.

The plasmas were produced by focussing a 700 mJ, 16 ns FWHM, laser pulse from a Q-switched Nd:YAG laser to a power density of ~ 10^{11} Wcm^{-2} onto a pure tin bulk target. The resulting time (~8 ns) and spectrally (Δλ ~ 0.01 nm) resolved EUV spectra are compared with atomic structure calculations, performed with the Cowan suite of codes [4], to determine the dominant ion stage as function of time.

Experimental set-up

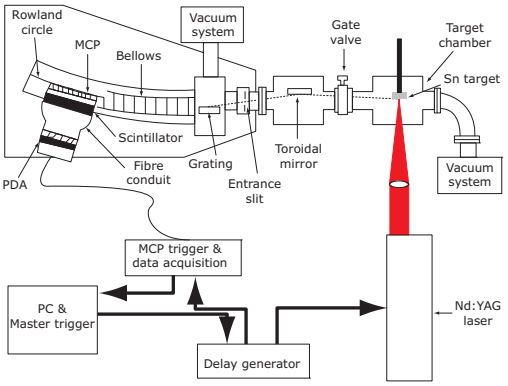

Figure 1: Schematic of the experimental set-up.

- The experimental set-up used to produce the plasmas under investigation is shown in **figure 1**.
- The plasmas under investigation are formed from a pure tin bulk target, by focussing a 700 mJ, 16 ns full width at half the maximum intensity, laser pulse from a Q-switched Nd:YAG laser (λ=1064 nm) to a power density of ~ 2 x10^{10} Wcm^{-2} onto the target.
- The radiation emitted is collected by a toroidal mirror and imaged onto the 20 mm entrance slit of a McPherson 2.2 m grazing incidence spectrograph, equipped with a 1200 groove/mm grating, giving a spectral resolving power of ~ 1000.
- The detector consists of a 40 mm microchannel plate (MCP) , which is coupled via a coherent fibre optic bundle to a 1024 pixel photodiode array (PDA).
- The microchannel plate can be gated to a width of 8 ns.
- The time delay between the plasma formation and the gating of the MCP was controlled *via* an electronic delay system. The definition of the time delays used are shown in **figure 2**.
- Further details of the experimental set-up can be found in [5].
- The experiment was repeated with the target rotated 45° towards the spectrometer.

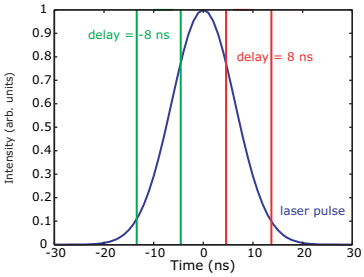

Figure 2: Definition of the time delays for the following figures.

Theoretical calculations:

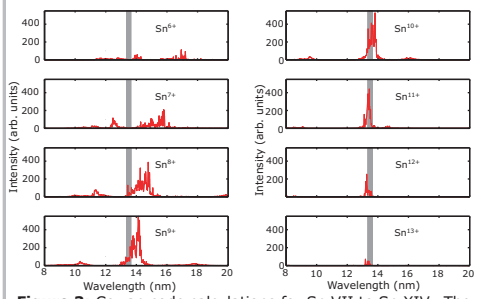

Figure 3: Cowan code calculations for Sn VII to Sn XIV. The shaded region represents the 2% bandwidth around 13.5 nm, referred to as the in-band region.

Table 1: Transitions included in Cowan code calculations, with n = 8, 7, 6, 5 and 4 for Sn VII, VIII, IX, X, and XI, respectively.

Even parity configurations	Odd parity configurations
$4p^64d^n$ (ground)	$4p^64d^{n-1}4f^1$
$4p^64d^{n-2}4f^2$	$4p^54d^{n+1}$
$4p^44d^{n+2}$	$4p^64d^{n-1}5f^1$
$4p^54d^n4f^1$	$4p^54d^n5s^1$
$4p^44d^{n+1}5s^1$	$4p^64d^{n-1}5p^1$
$4p^54d^n5p^1$	$4p^54d^n5d^1$
$4p^44d^{n+1}5d^1$	$4p^54d^n6s^1$
$4p^54d^n5f^1$	$4p^64d^{n-1}6p^1$
$4p^44d^{n+1}6s^1$	$4p^54d^n6d^1$
$4p^54d^n6p^1$	$4p^64d^{n-1}6f^1$
$4p^44d^{n+1}6d^1$	$4p^64d^{n-2}4f^16d^1$
$4p^54d^n6f^1$	$4p^64d^{n-2}4f^15d^1$

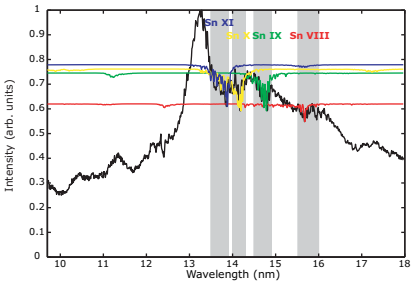

Figure 4: Comparison between Cowan code calculations and recorded spectrum to choose correct scaling factors. The bands shown in grey are used to determine the spectral region where each ion stage dominates

- The UTA in tin is due to 4p→4d and 4d→4f transitions, in ion stages containing an open 4d subshell.
- These transitions then merge to form a UTA of tens of thousands of individual lines [6], which must be parameterised statistically [7].
- Configuration interaction effects are important in determining the emitted spectrum and atomic structure calculations are preformed with the MCHF Cowan code [4].
- An example of configurations included in calculations are in **table 1**, and the resulting theoretical spectra are given in **figure 3**. Note only the $4p^64d^n \rightarrow 4p^54d^{n+1} + 4d^{n-1}4f + 4d^{n-1}5p$ transitions are plotted for clarity.
- These calculations can be improved by comparison with experimental data (**figure 4**), and the region where each ion stage dominates can be determined [8–10].

Results and discussion

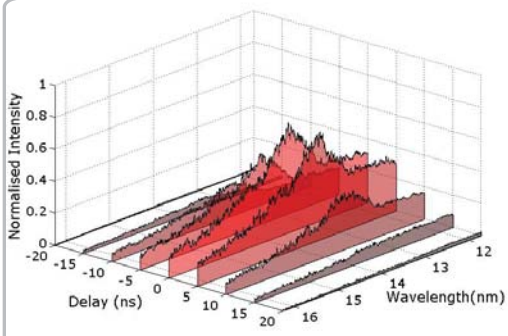

Figure 5: Time evolution of the EUV spectrum of tin for the parallel target geometry

- The EUV spectra recorded for tin as a function of time delay and wavelength are shown in **figures 5 & 6**, for the target parallel and at 45° to the spectrometer respectively, with the intensities normalised to the maximum recorded for the parallel case.
- Each spectrum corresponds to a gate of 8 ns, with 5 ns between each spectrum.
- As discussed in [11], for example, discrete features corresponding to each ion stage are not visible for spectra recorded at the angles used in this experiment.
- However, by using **figure 4**, where the regions dominated by individual ion stages were identified, integrated intensities of the contribution of Sn VIII to Sn X to the emission spectra recorded can be extracted.
- These integrated intensities are shown in **figure 7 & 8**, for the target parallel and at 45° to the spectrometer, as a function of time delay, along with the time evolution for the intensity of the 2% in-band region at 13.5 nm.
- It is observed, in agreement with [12, 13], that the EUV emission closely follows the profile of the laser pulse. This is shown more clearly in **figure 9**, where the laser pulse profile is shown, with the normalised in-band emission for both geometries overlaid.

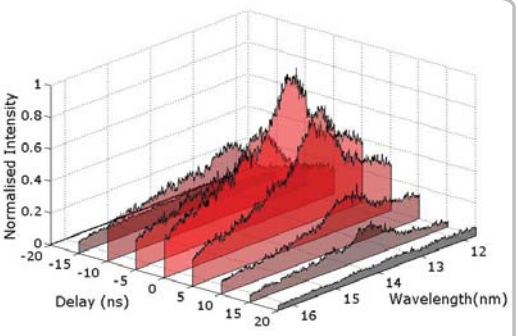

Figure 6: Time evolution of the EUV spectrum of tin for the 45° target geometry

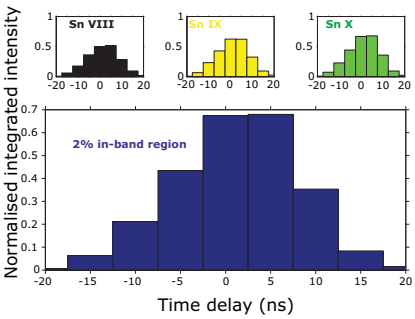

Figure 7: Time evolution of the integrated intensities of the wavelength regions dominated by ion stages Sn VIII to Sn X, and the evolution of the in-band intensity for the parallel target geometry

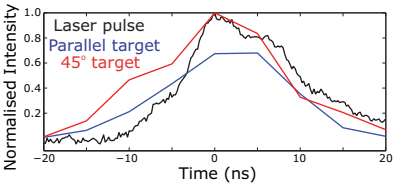

Figure 9: Time evolution of the integrated intensities of the in-band intensity for both geometries, overlaid with the temporal profile of the laser pulse used to form the plasmas

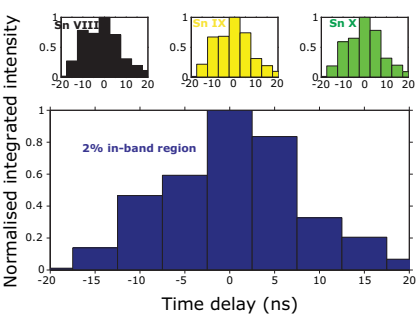

Figure 8: Time evolution of the integrated intensities of the wavelength regions dominated by ion stages Sn VIII to Sn X, and the evolution of the in-band intensity for the 45° target geometry.

References

[1] V. Baskshi, EUV Sources for Lithography, SPIE Press (2007)
[2] J. White *et al.*, J. Appl. Phys. 106, 113303 (2009)
[3] J. White *et al.*, J. Appl. Phys. 98, 113301 (2005)
[4] R. Cowan, The Theory of Atomic Structure and Spectra,University of California Press (1981)
[5] E. T. Kennedy *et al.*, Opt. Eng. 33, 3984 (1994)
[6] P. Mandelbaum *et al.*, Phys. Rev. A, 35, 5051 (1987)
[7] C. Bauche-Arnoult and J. Bauche, Physica Scripta T40, 58 (1992)
[8] P. Hayden, Ph. D. Thesis, UCD (2007)
[9] P. Hayden *et al.*, J. Appl. Phys. 99, 093302 (2006)
[10] O. Morris *et al.*, Appl. Phys. Lett. 91, 81506 (2007)
[11] P. Hayden *et al.*, Microelectronic Engineering 83 699–702 (2006)
[12] Y. Shimada *et al.*, Appl. Phys. Lett. 86 051501 (2006)
[13] H. Tanaka *et al.*, Appl. Phys. Lett. 87 041503 (2006)

Acknowledgements

The authors would like to thank Science Foundation Ireland, for funding under award 07/IN.1/I1771. Work done in frame of EU COST MP0601 Action and ERASMUS MUNDUS - EMJD - EXTATIC - FPA 2012-033 - EACEA programme.